Photodetachment dynamics of F_2^- in a strong laser field

Hannes Hultgren and Igor Yu. Kiyan
Physikalisches Institut, Albert-Ludwigs-Universität, D-79104 Freiburg, Germany
(Received 29 March 2011; published 18 July 2011)

The angle-resolved photoelectron spectrum of F_2^-, exposed to a strong infrared laser pulse, is significantly different from the spectrum of F^- obtained under the same experimental conditions. The experimental results are used to test the theory based on the molecular strong-field approximation. Both the dressed and the undressed versions of this theory fail to reproduce the F_2^- spectrum. One origin for this discrepancy is that photodetachment of F^- produced by strong-field dissociation of F_2^- needs to be considered.

DOI: 10.1103/PhysRevA.84.015401 PACS number(s): 32.80.Gc, 32.80.Rm

Ionization of atoms and molecules in a strong laser field represents a hot topic of recent studies on nonlinear interaction of matter with laser radiation. At high laser intensities, the photoelectron can gain substantially more energy from the field than necessary to overcome the ionization threshold. This gives rise to an above-threshold ionization (ATI) structure in electron emission spectra [1,2]. The energy spectrum is characterized by the electron ponderomotive energy U_p, which represents the kinetic energy of the electron quiver motion in the field averaged over the optical cycle. Angle-resolved photoelectron spectra carry valuable information used to identify mechanisms that govern the ionization process. For instance, the electron rescattering on its parent core is found to be responsible for the energy plateau, stretching along the polarization axis of a linearly polarized field, with a cutoff energy of $10U_p$. As another example, the nonmonotonic structure in angle-resolved spectra reveals the effect of quantum interference, which was clearly observed in recent experiments on strong-field photodetachment of atomic negative ions [3,4].

Among theories developed for description of the ionization process, the theory based on the strong-field approximation (SFA) [5] is the most fascinating, combining the power of prediction and simplicity. The approximation consists of neglecting the core potential in the final state. The final state is then represented by a Volkov wave function [6]. The SFA theory enables us to describe the phenomenon of ionization on a fundamental level, relating it to a coherent superposition of electron trajectories in the continuum [7–9]. In particular, the effect of quantum interference is intrinsically included in the final expression describing the ionization rate. In fact, the SFA theory was used in [3,4] to identify this effect in photoelectron spectra.

The SFA theory was recently extended to describe ionization of diatomic molecules [10–12]. Additional parameters, such as the molecular orientation and the symmetry of the initial electronic state, need to be considered in this case. The presence of two centers in a diatomic molecule gives rise to additional interference, related to a superposition of electron waves emitted from different centers. The dressing of the initial electronic state by the field represents an important issue here [12]. Similar to the standard atomic SFA, the undressed version of the molecular SFA [10–12] neglects the laser field in the initial state. Its dressed version is formulated in [12] by accounting for the difference in the electron potential energy at the two centers in the presence of the laser field. The dressing results in the phase shift $e^{i\mathbf{R}\cdot\mathbf{k}(t)}$ between waves emitted from different centers, where $\mathbf{R}$ is the internuclear distance, $\mathbf{k}_t = -e\int^t \mathbf{F}(t')dt'$ is the classical electron momentum due to the field, and e is the electron charge. This changes drastically the predictions of photoelectron distributions.

In the present Brief Report we aim to test the dressed and undressed versions of the molecular SFA experimentally. Analogously to the case of atomic ionization, molecular anions represent a well-suited system for this purpose. This is because the absence of the long-range Coulomb potential in negative ion detachment justifies applicability of the SFA approach. Below we present an angle-resolved photoelectron spectrum of F_2^- exposed to a laser pulse of 130 fs duration and 1300 nm wavelength. The field strength used in our experiment is of the order of the characteristic field experienced by the valence electron in F_2^-.

An added complexity in the present study is that interaction with the laser field can also initiate photodissociation of the molecular anion, generating F^- and F. Since a typical dissociation period ($\sim 10^{-14}$ s) is shorter than the pulse length used here, the dissociation products can subsequently interact with the pulse. Because subsequent photodetachment of F^- contributes to the photoelectron yield, in the present work we consider the dissociation channel as well. (Subsequent ionization of F can be disregarded since the ionization potential of the fluorine atom is considerably higher than its electron affinity). Our experiment cannot distinguish between electrons detached from F_2^- and F^-. Therefore, we have separately recorded a photoelectron spectrum of F^-, exposed to the same laser pulse as F_2^-.

Both F_2^- and F^- are extracted from a glow discharge source operated with a gas mixture of NF_3 (10%) and Kr (90%). Negative ions, accelerated to a kinetic energy of 3 keV, pass through a Wien filter that selects either the F_2^- or F^- component of the ion beam. A typical ion current transmitted into the interaction region is 15 nA of F_2^- or 150 nA of F^-. The mass-selected ion beam is intersected with the laser beam inside an electron imaging spectrometer (EIS) operated in the velocity mapping regime. Linearly polarized laser pulses of 1300 nm wavelength are generated in an optical parametric amplifier (OPA) pumped with a mode-locked Ti:sapphire laser system at a repetition rate of 1 kHz. The output of the OPA is focused with a 15-cm-focal-length lens into the interaction region. A focus size of 46 μm (full width at half maximum) and a pulse duration of 130 fs are measured with the standard

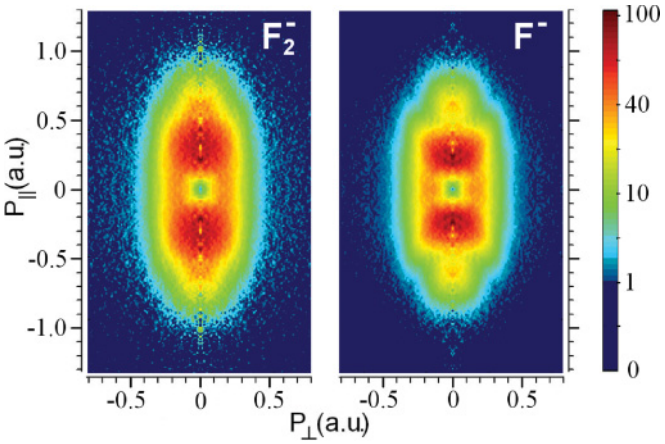

FIG. 1. (Color online) Momentum distribution of photoelectrons detached from F_2^- (left) and F^- (right) in a laser field of 1300 nm wavelength and 3.4×10^{13} W/cm^2 peak intensity. $p_\perp$ and $p_\parallel$ represent the momentum components perpendicular and parallel to the laser polarization axis, respectively.

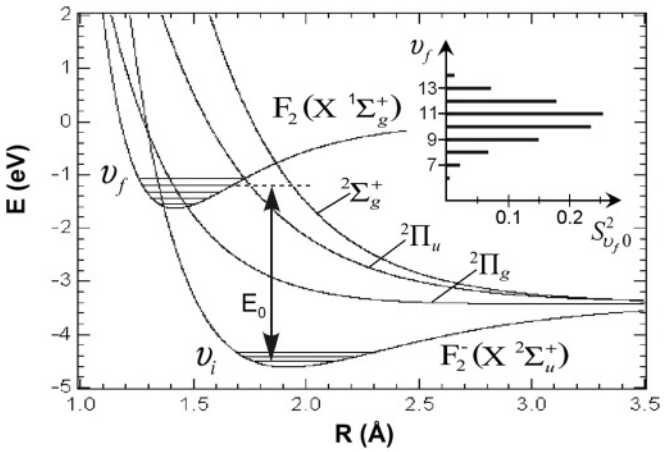

FIG. 2. Potential energy curves of electronic states of F_2^- and the ground electronic state of F_2. v_i and v_f are the vibrational quantum numbers of F_2^- and F_2 vibrational states, respectively, E_0 denotes the threshold energy for a given $v_i \to v_f$ transition. The inset shows the squared overlap of nuclear wave functions, $S^2_{v_f v_i}$, for $v_i = 0$ and different v_f values.

beam diagnostic tools. Assuming a Gaussian shape of the spatiotemporal intensity distribution, the peak intensity in the focus is determined to be 3.4×10^{13} W/cm^2. The acquisition of F_2^- and F^- spectra is broken in alternating sequences in order to eliminate uncertainties caused by a long-term drift of the laser and ion beams. This ensures that both F_2^- and F^- negative ions are exposed to the same laser pulse. The images recorded with the EIS are processed using a conventional Abel inversion routine, which reconstructs the angle-resolved momentum distribution of photoelectrons emitted from the interaction region. Further details on the experimental setup and the image processing can be found elsewhere [4].

The angle-resolved photoelectron spectra of F_2^- and F^- are presented in Fig. 1 in the $(p_\perp, p_\parallel)$ coordinates, where $p_\perp$ and $p_\parallel$ are the momentum components perpendicular and parallel to the laser polarization axis, respectively. The distributions shown in Fig. 1 differ significantly. In particular, the F_2^- spectrum is broader along the polarization axis and it does not exhibit the nonmonotonic structure at higher momenta $p_\parallel$, which is well pronounced in the F^- spectrum. This structure, appearing as two islands on the $p_\parallel$ axis at $p_\parallel = \pm 0.6$ a.u., is due to the effect of quantum interference, which is discussed in detail in [4]. The considerable difference of the F_2^- and F^- spectra indicates that F_2^- does not dissociate at low intensities on the leading edge of the laser pulse and, thus, is exposed to a strong field.

Let us now describe photodetachment of F_2^- using the molecular SFA. The differential detachment rate in the laser field $\mathbf{F}(t) = \mathbf{F}\cos\omega t$ is given by the sum over n-photon channels [7] (atomic units are used throughout),

$$dw = 2\pi \sum_{n \geqslant n_0} |A_{\mathbf{p}n}|^2 \delta\left(\frac{p^2}{2} + U_p + E_0 - n\omega\right) \frac{d^3p}{(2\pi)^3}, \quad (1)$$

where $A_{\mathbf{p}n}$ is the n-photon transition amplitude to the final continuum state characterized by the electron momentum vector $\mathbf{p}$, n_0 is the minimum number of photons needed to overcome the ponderomotively shifted threshold, E_0 is the threshold energy, $U_p = F^2/(4\omega^2)$ is the electron ponderomotive energy in a linearly polarized laser field, and ω and F are the laser frequency and the field strength, respectively. The δ function accounts for the energy conservation rule. For a given final vibrational state v_f of the residual F_2 molecule, the threshold energy is $E_0 = E_{v_f} - E_{v_i}$, where v_i and v_f denote the vibrational quantum numbers of the initial state of F_2^- and the final state of F_2, respectively, and E_{v_i} and E_{v_f} are the energies of these states. This is illustrated in Fig. 2, which shows the potential curves of the ground electronic states $^2\Sigma_u^+$ and $^1\Sigma_g^+$ of the anion and its parent molecule, respectively. The potential curves are obtained from Ref. [13]. The fundamental vibrational frequency of F_2^- in its ground electronic state is 450 cm^{-1} [13]. One can easily estimate that only a few low vibrational states can be populated according to the Boltzmann distribution at a typical gas temperature of glow discharge. As an approximation, we therefore consider that all negative ions are produced in the lowest vibrational state $v_i = 0$.

Following results of Ref. [12], the transition amplitude for an initial state of ungerade symmetry has the form

$$A_{\mathbf{p}n} = -\frac{\omega}{2\pi} S_{v_f v_i} \sum_{s=\pm 1} s \int_0^T e^{\frac{i}{2}s(\mathbf{p}+\eta\mathbf{k}_t)\cdot\mathbf{R}_0} \tilde{\psi}(\mathbf{p}+\mathbf{k}_t) \times \left(E_0 + \frac{(\mathbf{p}+\mathbf{k}_t)^2}{2}\right) e^{\frac{i}{2}\int^t (\mathbf{p}+\mathbf{k}_t)^2 d\tau + iE_0 t} dt, \quad (2)$$

where the sum accounts for contributions from the two centers of the diatomic anion, $\mathbf{R}_0$ defines the molecular axis and the equilibrium distance between nuclei in F_2^-, $S_{v_f v_i}$ is the overlap of nuclear wave functions of F_2^- and F_2, $T = 2\pi/\omega$, and $\tilde{\psi}(\mathbf{q})$ is the Fourier transform of the atomic orbital $\psi(\mathbf{r})$ which composes the highest occupied molecular orbital (HOMO) of σ_u symmetry in F_2^-. The index η in Eq. (2) defines whether the initial state is considered to be dressed ($\eta = 0$) or undressed ($\eta = 1$).

The values of $S^2_{v_f v_i}$ for $v_i = 0$ and different v_f are presented in the inset of Fig. 2. It shows that the overlap of nuclear wave

functions has a peak at $\nu_f = 11$. The large value of ν_f is due to the rather large difference in equilibrium positions of nuclei in F_2^- and F_2, as one can see from the potential energy curves in Fig. 2. The distribution of $S^2_{\nu_f \nu_i}$ over ν_f is rather narrow, and the energy interval between vibrational levels of F_2 in the vicinity of $\nu_f = 11$ is small ($\approx$540 cm^{-1}) in comparison with the photon energy. Thus, the population spread over different final vibrational states can be disregarded, and we consider the formation of F_2 only in the $\nu_f = 11$ state and assign 1 to $S_{\nu_f \nu_i}$ in Eq. (2). The threshold energy E_0, explicitly defined by the difference $E_{\nu_f=11} - E_{\nu_i=0}$, is 3.965 eV. Five photons are required to overcome this threshold.

We evaluate Eq. (2) analytically by using the method of steepest descent in the same way as described in [7]. In order to simplify this task, the two-center zero-range potential model [14] is used for the description of the electronic state. In this model, the HOMO wave function of F_2^- can be represented analytically as $\Psi(\mathbf{r}) = \psi(\mathbf{r} + \mathbf{R}_0/2) - \psi(\mathbf{r} - \mathbf{R}_0/2)$, where

$$\psi(\mathbf{r}) = C\frac{e^{-\kappa r}}{r} Y_{10}(\theta_m, \phi_m), \tag{3}$$

$C = 0.701$ is the normalization coefficient, Y_{10} is the spherical harmonic, the spherical angles (θ_m, ϕ_m) are defined with respect to the molecular axis, and $\kappa^2/2$ is the vertical electron affinity defined as the energy difference between the potential curves in Fig. 2 at the equilibrium distance $R_0 = 1.937$ Å. In the spherical coordinates (θ, ϕ) with respect to the laser polarization axis, the angular part of the atomic orbital in Eq. (3) can be represented as

$$Y_{10}(\theta_m, \phi_m) = \cos(\alpha) Y_{10}(\theta, \phi) + \sin(\alpha)\frac{1}{\sqrt{2}} \times [Y_{1-1}(\theta, \phi) - Y_{11}(\theta, \phi)], \tag{4}$$

where α is the angle between the molecular axis and the polarization axis. Since the molecular anions are randomly oriented in the laser focus, the photodetachment rate is averaged over α and ϕ.

The simulation routine of photoelectron spectra is described elsewhere [4]. It involves integration of the electron yield over the spatiotemporal intensity distribution in the laser focus and accounting for depletion of negative ions during their interaction with the field. Results of simulations are presented in Fig. 3. Comparison of the predicted distributions with the measured spectrum of F_2^- (see Fig. 1) shows that neither the dressed nor the undressed version of the molecular SFA agree with experiment. Both simulated spectra exhibit a nonmonotonic structure, caused by the effect of quantum interference, which consists of two maxima lying on the laser polarization axis. As expected, this structure is very different in the dressed and undressed versions of the molecular SFA. On closer inspection of the predicted spectra, one can see that the position of the broad maximum in the experimental spectrum is not reproduced in either simulation. This is quantitatively illustrated in Fig. 4, which compares the measured and predicted distributions of photoelectrons emitted along the laser polarization axis. We would like to point out that the low-energy contribution to the spectrum is suppressed in the dressed version of the molecular SFA (see Figs. 3 and 4). This result is explained in [12] as being due to the effect of two-center interference.

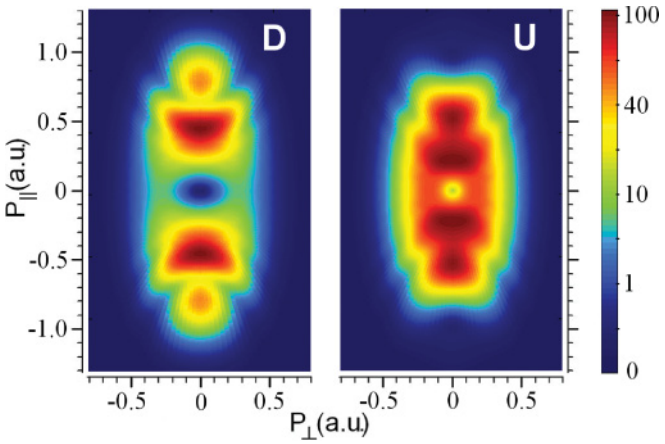

FIG. 3. (Color online) Photoelectron distributions of F_2^- predicted by the dressed (left) and undressed (right) versions of the molecular SFA.

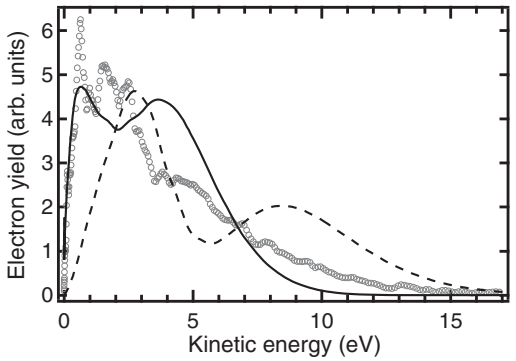

FIG. 4. Energy distribution of photoelectrons emitted from F_2^- along the laser polarization axis. Circles represent experiment, solid and dashed lines show predictions by the undressed and dressed versions of the molecular SFA, respectively. The curves are normalized according to the integrated yield.

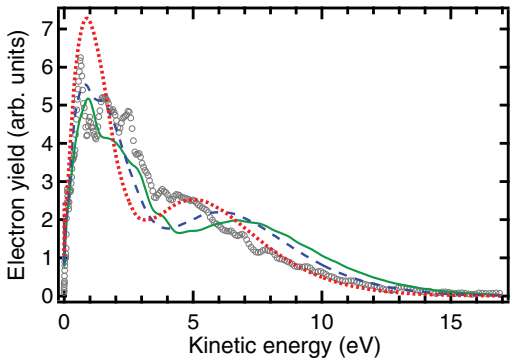

FIG. 5. (Color online) Comparison of the experimental energy distribution shown in Fig. 4 (circles) with predictions by the model that assumes strong-field dissociation of F_2^- followed by photodetachment of F^-. Calculations are performed for different initial times (see text): $-\sigma_t$ (dotted line), $-\sigma_t/2$ (dashed line), and 0 (solid line). The curves are normalized according to the integrated yield.

As an alternative description of the F_2^- spectrum, let us consider that dissociation of F_2^- occurs at high laser intensities and is followed by photodetachment of the created F^-. Thus, the atomic anions appear in the laser focus at a time t_0, which is close to the center of the temporal pulse envelope, and their detachment during the rest of the pulse ($t > t_0$) constitutes the electron yield. Photoelectron spectra of F^- are calculated by using our simulation routine [4] for different initial times $t_0 = -\sigma_t$, $-\sigma_t/2$, and 0. Here $\sigma_t = 79$ fs is the measured Gaussian width of the temporal intensity profile $I(t) = I\exp(-t^2/\sigma_t^2)$, and the peak of the pulse is at $t = 0$. The calculated energy distributions of electrons detached along the laser polarization axis are compared with the measured spectrum of F_2^- in Fig. 5. One can see that the distribution width is larger when t_0 is closer to the center of the pulse. This is because the negative ions are less depleted before they experience higher intensities generating photoelectrons of higher kinetic energies. The broadest electron distribution is obtained for $t_0 = 0$, since in this case the created F^- ions are immediately exposed to the peak intensity. However, even for $t_0 = 0$ the simulated spectrum is still narrower than the measured distribution at low energies ($\lesssim$3.5 eV), while the simulation overestimates the higher-energy part of the spectrum. Each predicted distribution shown in Fig. 5 possesses a well-pronounced nonmonotonic structure caused by the quantum interference effect [4]. This structure, however, is not resolved in the experimental spectrum.

Considering that F^- ions are created by dissociation over a range of values of t_0, the predicted distribution should be averaged over t_0. Figure 5 reveals that, depending on t_0, the simulation can either reproduce the high-energy tail of the experimental spectrum or better reproduce its low-energy part. Therefore, a superposition of curves calculated for various t_0 cannot describe the experimental distribution in the entire energy range and the contribution from strong-field detachment of F_2^- needs to be reconsidered as well.

Summarizing, photodetachment of F_2^- in a strong laser field reveals complicated dynamics, involving both direct strong-field detachment of the molecular anion and detachment of F^- created in the laser focus by strong-field dissociation. A coincidence technique (e.g., similar to the one developed in [15]), making it possible to distinguish between electrons produced in these processes, is required for the experimental test of the molecular SFA. We believe that our results will initiate the development of more comprehensive methods, accounting for the complexity of molecular orbitals, where detachment and dissociation are considered as competing processes and the population dynamics of the molecular and atomic anions in the laser focus is taken into account.

The authors greatly appreciate fruitful discussions with Professor Hanspeter Helm. This work is supported by the Deutsche Forschungsgemeinschaft, Grant No. KI 865/3-1.

[1] L. F. DiMauro and P. Agostini, Adv. At. Mol. Opt. Phys. **35**, 79 (1995).
[2] W. Becker *et al.*, Adv. At. Mol. Opt. Phys. **48**, 35 (2002).
[3] I. Yu. Kiyan and H. Helm, Phys. Rev. Lett. **90**, 183001 (2003).
[4] B. Bergues, Z. Ansari, D. Hanstorp, and I. Y. Kiyan, Phys. Rev. A **75**, 063415 (2007).
[5] L. V. Keldysh, Zh. Eksp. Teor. Fiz. **47**, 1945 (1964) [Sov. Phys. JETP **20**, 1307 (1965)].
[6] D. M. Volkov, Z. Phys. **94**, 250 (1935).
[7] G. F. Gribakin and M. Yu. Kuchiev, Phys. Rev. A **55**, 3760 (1997).
[8] R. Kopold, W. Becker, and M. Kleber, Opt. Commun. **179**, 39 (2000).
[9] A. Gazibegović-Busuladžić, D. B. Milošević, and W. Becker, Phys. Rev. A **70**, 053403 (2004).
[10] T. K. Kjeldsen and L. B. Madsen, J. Phys. B **37**, 2033 (2004).
[11] A. Jarón-Becker, A. Becker, and F. H. M. Faisal, Phys. Rev. A **69**, 023410 (2004).
[12] D. B. Milošević, Phys. Rev. A **74**, 063404 (2006).
[13] J. G. Dojahn, E. C. M. Chen, and W. E. Wentworth, J. Phys. Chem. **100**, 9649 (1996).
[14] R. Kopold, W. Becker, and M. Kleber, Phys. Rev. A **58**, 4022 (1998).
[15] K. A. Hanold *et al.*, Rev. Sci. Instrum. **70**, 2268 (1999).